Research Article DOI: https://doi.org/10.64862/ajeg.2026.301.03.308 Open Access

Landslide Susceptibility Assessment along the Hilly Coastal Corridor of Cox's Bazar-Teknaf, Bangladesh

Muqit Ajmain Shahriyar[1*], Md. Abdul Malek[1], Md. Younus Hider[1], Tasmim Banu[1], and Md. Mahedi Hasan[1]

[1]Department of Geology and Mining, University of Rajshahi, Rajshahi 6205, Bangladesh

(*Corresponding E-mail: muqit.ajmain2001@gmail.com)

Received: December 20, 2025, Accepted: May 28, 2026

Abstract: **The southeastern coastal cliffs of Bangladesh, extending from Cox's Bazar to Teknaf, are highly susceptible to landslides due to steep terrain, intense monsoonal rainfall, and increasing anthropogenic disturbances. This study presents an integrated landslide susceptibility assessment by combining the knowledge-based Analytic Hierarchy Process (AHP) and the data-driven Frequency Ratio (FR) model to identify spatial patterns of landslide. A landslide inventory comprising 55 documented landslide locations was prepared using NASA Global Landslide Catalog data and high-resolution Google Earth imagery. Ten conditioning factors- elevation, slope, aspect, curvature, soil type, geomorphology, rainfall, drainage density, distance from roads, and Normalized Difference Vegetation Index (NDVI) were derived from satellite imagery and geospatial datasets and synthesized within a Geographic Information System (GIS) environment to generate susceptibility maps. Model performance was evaluated using Receiver Operating Characteristic (ROC) curves and the Area Under the Curve (AUC) metric. The AHP model demonstrated strong predictive capability with an AUC value of 0.859, classifying 63.48% of the study area as moderate susceptibility and identifying 1.06% as high-susceptible zones, primarily along the Teknaf hill tracts. In contrast, the FR model exhibited moderate accuracy (AUC = 0.688) and produced a more detailed five-class susceptibility map, delineating 4.35% of the area as high to very high susceptible. Both models consistently indicate that critical landslide susceptibility is concentrated along the coastal cliffs of Teknaf and parts of the hilly terrain in Ukhiya. These findings have important implications for infrastructure safety, particularly the Marine Drive corridor, and for the densely populated Rohingya refugee settlements, where unstable slopes pose significant hazards. The comparative application of AHP and FR framework offers a cost-effective and transferable approach for landslide susceptibility assessment and disaster mitigation in data-scarce, high-hazard region.**

Keywords: ***Analytic Hierarchy Process (AHP), Frequency Ratio, Landslide Inventory, Multi-Criteria Decision Analysis, Disaster Risk Reduction.***

Introduction

Landslides are the gravity-driven movements of soil and rock on slopes. Most modern geomorphology sources say, a landslide as the movement of a mass of rock, debris, or earth down of a slope under gravity (Turner, 2018; Wubalem, 2021). They are among the most frequent geo-hazards in mountainous regions and cause substantial loss of life and property worldwide.

Global Study says that, about 4862 fatal non-seismic landslides killed 55997 people in 2004-2016, heavily concentrated in Asia (Froude et al., 2018). In the USA, estimated annual landslide frequencies range from ~0.002 to 29 landslides per 1000 km^2 per year (Luna et al, 2025). This hazard occurs with a family of gravity-driven movements that include falls, topples, slides, spreads, flows, and their complex combinations, acting through stages of failure, movement and deposition (Varnes, 1978). Shear failure happens along a surface or in a shear zone when driving stress exceeds shear strength (Petley et al., 2002; Cuomo, 2020). Post failure movement occurs acceleration, possible transition from slide to flow and entrainment of more material (Cuomo, 2020; Tian et al., 2020).

Most of the landslides occur in mountainous topography on moderate-steep, concave mid-upper slopes, especially in zones dissected by rivers or roads; in flatter or low-relief terrain, landslides are much less common. A global analysis of fatal landslides shows that ~70% of natural landslides and ~44% of human-triggered ones occur in mountainous areas in tropical and temperate regions (Fidan et al., 2024). Most of the cases natural-factor landslides tend to initiate in the higher parts of the topographic profile, at higher elevations and steeper slopes with little human disturbance (Carrara, 1983; Fidan et al., 2024). Some studies also find that while steeper slopes are more susceptible, extremely steep slopes may have thinner, more stable soils, so landslide erosion can peak on near-threshold but not the very steepest slopes (Prancevic et al., 2020).

Bangladesh comprises up a large portion of the Bengal Basin, and its coastal areas undergo landslides of any dimension (Rahman et al., 1995). In Bangladesh, landslide-vulnerable areas mainly concentrated in the southeastern and some northeastern hilly districts, especially around Chattogram and Cox's Bazar which are identified as landslide-prone districts based on 2000-2018 catalog (Sultana, 2020). Steep, deforested slopes (often 12-30° or more, 60-200 m elevation) with sandy/loamy soils in Cox's Bazar and Chattogram are

the most vulnerable factor for landslide hazard (Chowdhury et al., 2023; Nahar et al., 2025; Islam et al., 2024). Intense monsoon rainfall saturates weak sandy soils on steep, cut, and deforested slopes, especially around roads, camps, and informal settlements accelerate landslide. In Cox's Bazar (Ramu-Ukhiya-Teknaf), June rainfall shows a strong statistical correlation with monthly landslide incidence (Nahar et al., 2025). High topographic wetness and stream power indices (areas where runoff converges) are strongly associated with failures because they focus infiltration and erosion (Islam et al., 2024; Fuad et al., 2024). Between Cox's Bazar and Teknaf (the Teknaf Peninsula), the land is a narrow ridge of low hills flanked by the Bay of Bengal to the west and the Naf River/floodplains to the east. These hills form a dissected, erosion-prone landscape with strong relief over short distances. In Cox's Bazar district, most hills are ~100-300 m high (Ahmed et al., 2020) and the Ramu-Ukhiya-Teknaf belt, high landslide vulnerable sites are typically at ~90-180 m elevation (Nahar et al., 2025). Hill materials make the area influencing for its unconsolidated or weakly cemented sand, silt and shale, giving high erodibility and frequent shallow landslides when disturbed (Nahar et al., 2025; Kamal et al., 2022; Ahmed et al., 2020).

Recent devastating landslides between Cox's Bazar and Teknaf have concentrated on the Ukhiya-Teknaf Rohingya camp corridor and neighboring host villages, particularly in 2017, 2019, and 2021, displacing thousands and claiming multiple lives throughout each major monsoon season. At June 2017, landslides occur at least 160 deaths in Cox's Bazar district and adjacent hills (Ahmed et al., 2020). At July 2019, 355 mm rain happened over 72 hours and causes 26 landslides, 1 death, ~4,500 people left homeless (Sami et al., 2024). Besides geologic factors, road cuts, building platforms, and quarrying over-steepen slopes and remove support at the toe, making failure much more likely during rain (Skilodimou et al., 2018).

At 2024, regional assessment integrating hazard (susceptibility) and social vulnerability for all southeast Bangladesh finds landslide risk highest in Teknaf, Ukhiya and Ramu upazilas; Cox's Bazar district is second only to Chattogram in overall risk (Sultana et al., 2024). Although numerous landslide susceptibility studies have been conducted in the Chattogram Hill Tracts and surrounding regions (Rabby et al., 2020), relatively few investigations have specifically focused on the Cox's Bazar-Teknaf coastal hill corridor, where rapid infrastructure development, extensive road-cutting activities, and the establishment of large refugee settlements have substantially altered slope stability conditions. Previous studies have commonly applied either statistical or knowledge-based approaches independently; however, a comparative assessment of the Analytic Hierarchy Process (AHP) and Frequency Ratio (FR) models for this coastal environment remains limited. Furthermore, recent changes in land use, vegetation cover, and anthropogenic disturbances necessitate updated susceptibility assessments. Therefore, this study contributes by (i) developing updated landslide susceptibility maps using recent geospatial datasets, (ii) comparing the predictive performance of expert-based and data-driven approaches, and (iii) identifying critical landslide hotspots that directly threaten transportation corridors, settlements, and refugee camps within southeastern Bangladesh to support disaster preparedness and land-use planning.

Geographic and environmental settings

The study area is situated in the southeastern part of Bangladesh along the longest sea beach and the Marine Drive extending roughly between 20°52'-21°25'N latitude and 91°58'-92°18'E longitude shown in Figure 1. It encompasses selected coastal and hilly terrain within the Ramu, Ukhiya, and Teknaf upazilas of Cox's Bazar district. In this area, the exposed hill rocks belong to the Cenozoic Tertiary succession of the Chittagong-Tripura Folded Belt. Regionally, it includes Bhuban Formation (Miocene), Boka Bil (Miocene), Tipam Sandstone + Girujan Clay (Pliocene), Dupi Tila (Plio-Pleistocene), and Recent alluvium (Khanam et al, 2020; Hossain et al., 2025). The Cox's Bazar-Teknaf cliff is mainly dominated by sandstone and shale. Tertiary sandstone-shale successions, weathered at some part of the folded belt that continues into Cox's Bazar area (Hossain et al., 2025). The hilly terrain rises progressively eastward to hundreds of meters in the regional hill belt. (Saddam et al., 2025). In Ramu, Ukhiya and Teknaf upazilas, high landslide-vulnerable hillslopes commonly have steep slopes of about 12-21° and elevations of 89-177 m (Nahar et al., 2025). The natural hilly terrain mostly from gentle 6-12° slopes to steeper 12-21° slopes, but human-modified camp and cut slopes often reach 40-60°, where stability problems and landslides are common (Kamal et al., 2023; Sami et al., 2024). Drainage density in this area is high enough to strongly control erosion, landslides, and water availability. Such networks are mainly dendritic and dominated by numerous short 1st- 3rd order streams on steep slopes that rapidly convey runoff (Chowdhury, 2024). Streams in nearby Chattogram basins (Sangu-Matamuhuri) have high wet-season peak flows and low dry-season baseflow; over a 25-year period, wet-season runoff has increased and dry-season flow has decreased, suggesting flashier behavior and an increasing danger of water scarcity (Rudra et al., 2023).

This hilly zone of Bangladesh lies in humid tropical monsoon belt. It has a marked seasonal cycle with very high rainfall and warm temperatures year-round, and both rainfall and temperature are increasing over recent decades. The Teknaf peninsula is very wet, with typical annual rainfall around 3000-4000 mm, with ~15 °C in winter and ~33 °C in summer (Moslehuddin et al., 2018). Long-term analyses (1950–2023) show increasing annual and seasonal rainfall at Cox's Bazar and Teknaf, though seasonal trends can be irregular and partly non-significant (Suhan et al., 2025). Vegetation in the

Cox's Bazar-Teknaf hill zone ranges from natural semi-evergreen hill forests and coastal Casuarina belts to species-rich homestead agroforests and mangrove-wetland mosaics. Himchari National Park of Cox's Bazar contains 88 tree species (961 stems, 457 stems/ha), with high diversity but dominance of plantation/introduced trees like Acacia auriculiformis, Tectona grandis, Gmelina arborea, Casuarina equisetifolia alongside native species (Hossen et al., 2020). In Teknaf 73 plant species and very high densities (~4000 plants/ha) have been recorded, providing timber, fuelwood, fruits and cyclone protection and storing substantial carbon (117 Mg C/ha) (Nath et al., 2015).

Population growth is highly concentrated in Ukhiya and Teknaf, especially around refugee settlements and growth corridors along roads and upazila centers. Geospatial evidence suggests the regional population-density dimension increased at about 9431 persons/year, alongside a rural-to-urban transition driven by refugee settlement expansion. More than one million refugees have settled mainly in rural and forested areas because of their proximity to the Myanmar border and accessible transport routes (Islam et al., 2023). This population growth has accelerated infrastructure development along secondary highways, camp areas, and modified hill slopes, increasing exposure to landslides, flooding, and heat stress. Development for camps, roads, sanitation, and markets has expanded into environmentally sensitive terrain (Mohiuddin et al., 2025), resulting in the conversion of forest-dominated landscapes into settlements, camps, roads, and other built-up areas (Hossain et al., 2021; Mazumder et al., 2024).

Overall, the Cox's Bazar-Teknaf hilly region is characterized by clustered population growth, infrastructure concentrated in hazard-prone corridors, and extensive forest conversion to settlement and camp-related land uses.

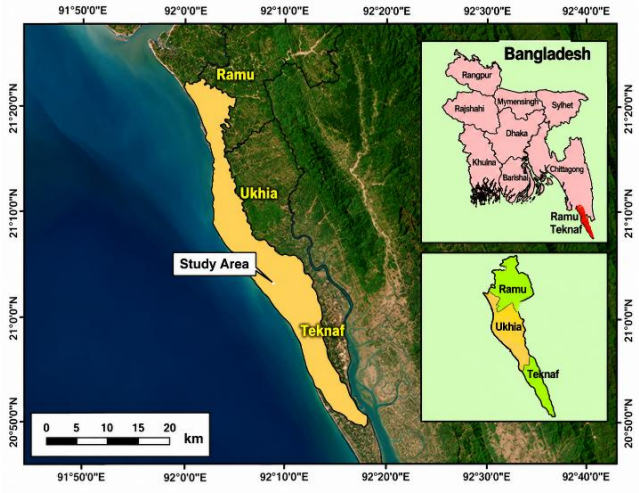


Figure 1, Location map of the study area showing the Cox's Bazar-Teknaf coastal hill corridor and major administrative boundaries.

Methodology

The study maps the landslide susceptibility of the Cox's Bazar-Teknaf coastal cliff using the Analytic Hierarchy Process (AHP) and Frequency Ratio (FR) approach. An outline of the methodological approach is given in (Figure 2). The Analytic Hierarchy Process (AHP) was used to assess the relative weights of the landslide conditioning factors based on expert judgment and their contribution to the occurrence of landslides. At first a hierarchical structure with the objective, criteria, and possibilities was created. The selected conditioning factors included elevation, slope, aspect, curvature, drainage density, soil type, distance from road, annual rainfall, geomorphology, and NDVI. Then, a weighted overlay technique was applied using ArcGIS 10.8 to generate the AHP-based landslide susceptibility map, which was subsequently classified into different susceptibility zones. To ensure the reliability of expert judgments, the consistency of the pairwise comparisons was evaluated using the Consistency Index (CI) and Consistency Ratio (CR) (Yang et al., 2022). On the other hand, Frequency Ratio (FR) method is a widely used bivariate statistical technique for landslide susceptibility assessment and other natural hazard studies (Lee et al., 2006). It evaluates the spatial relationship between historical landslide occurrences and landslide conditioning factors such as slope, aspect, geology, soil type, drainage characteristics, geomorphology, rainfall, and vegetation indices. The frequency ratio for each class was calculated as the ratio of the percentage of landslide pixels within a given class to the percentage of the area occupied by that class. Finally, the FR values of all factor classes were spatially assigned and summed to generate the FR-based landslide susceptibility map using ArcGIS 10.8. After generating the AHP- and FR-based models, the landslide susceptibility results were analyzed and validated using the receiver operating characteristic (ROC) curve and the area under the curve (AUC).

Dataset for the study

The landslide susceptibility analysis incorporated a set of topographic, environmental, climatic, and anthropogenic conditioning factors. The datasets included both raster and vector data acquired from USGS Earth Explorer, Landsat 8, and other relevant and authoritative sources. The selected datasets, their respective sources, spatial resolutions/scales, and classification methods are summarized in Table 1.

Topographic conditioning factors, including elevation, slope, aspect, curvature, and drainage density, were derived from the Digital Elevation Model (DEM). Environmental and anthropogenic factors, including soil type, geomorphology, and distance from roads, were prepared from relevant ancillary vector datasets. Annual rainfall data were obtained from the Climatic Research Unit (CRU) gridded climate dataset in NetCDF format, provided by the University of East

Anglia, with a spatial resolution of 0.5° × 0.5° (approximately 50 km). Landsat 8 imagery was used to derive the Normalized Difference Vegetation Index (NDVI), which was incorporated as an additional conditioning factor in the landslide susceptibility analysis.

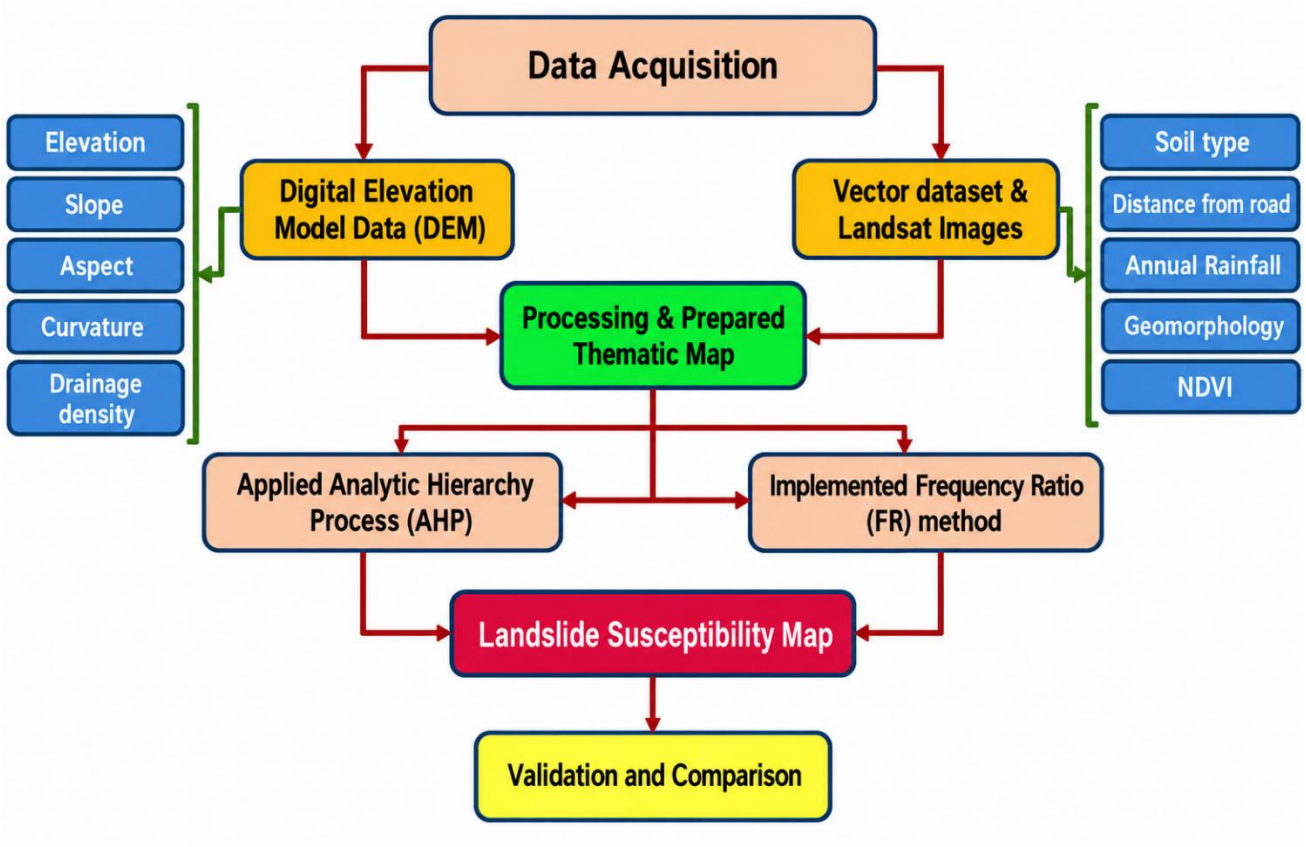


Figure 2, Methodological framework of the study.

Table 1, Datasets and parameters used for landslide susceptibility mapping.

Datasets	Parameters	Source	Acquisition Date	Scale	Classification method
Digital Elevation Model (DEM)	Elevation	USGS Earth Explorer	2014/09/23	30m×30m	Natural break
	Slope				
	Aspect				
	Curvature				
	Drainage Density				
Vector Datasets	Soil type	Open Source data	2023/09/04		Natural break
	Distance form road				
	Geomorphology				
NetCDF	Annual Rainfall	Climatic Research Unit (CRU)	Temporal coverage: January-December 2024		
Landsat Image	NDVI	USGS Earth Explorer	2025/03/13		

Before thematic layer generation, all spatial datasets were preprocessed within the ArcGIS 10.8 environment to ensure spatial consistency. All raster and vector datasets were projected to the World Geodetic System 1984 (WGS 84), Universal Transverse Mercator (UTM) Zone 46N coordinate reference system, clipped to the

study area boundary, and converted to a uniform raster format with a spatial resolution of 30 × 30 m. Topographic parameters, including elevation, slope, aspect, curvature, and drainage density, were derived from the Digital Elevation Model (DEM) using standard Spatial Analyst tools. The Euclidean Distance tool was used to generate the distance-from-road layer, while NDVI was calculated from Landsat imagery using the standard normalized difference equation.

Continuous variables were classified using the Jenks Natural Breaks method to preserve inherent data variability, whereas categorical variables such as soil type and geomorphology retained their original thematic classes. All thematic layers were subsequently standardized to ensure compatibility for AHP and FR-based landslide susceptibility modelling.

Landslide inventory database

A comprehensive landslide inventory database was prepared by integrating landslide occurrence records from the NASA Global Landslide Catalog with additional landslide locations identified through visual interpretation of high-resolution Google Earth imagery. The final inventory comprised 55 verified landslide locations, obtained from the NASA Global Landslide Catalog and supplemented by landslide locations interpreted from Google Earth imagery. All inventory points were carefully examined to eliminate duplicate records and ensure positional consistency before being incorporated into the GIS database. The landslide inventory served as the basis for susceptibility modelling, while model performance was evaluated using Receiver Operating Characteristic (ROC) analysis. The spatial distribution of the inventoried landslides covers the major hilly areas of the Cox's Bazar–Teknaf coastal corridor and provides the fundamental database for landslide susceptibility modelling.

Landslide conditioning factors

For this study, ten conditioning factors were selectively chosen based on a review of the literature, reliability, data accessibility, and their importance to the prevalence of landslides illustrated into (Figure 3 and Figure 4). Identifying and analyzing landslide conditioning factors is a crucial step in landslide susceptibility assessment, as these factors control slope instability and determine the spatial distribution of landslide occurrences.

Conditioning factors do not directly trigger landslides but create favorable conditions that increase the likelihood of failure when triggering events. Each conditioning factor was compiled into a raster format with a spatial resolution of 30 × 30 m in order to assure consistency in data analysis (Fuad et al., 2024).

To categorize the data, we employed the Jenks natural breaks method in the ArcGIS software. This approach facilitates the objective identification of important trends and clusters.

The ten conditioning factors were selected based on their widespread application in previous landslide susceptibility studies, their physical relevance to slope instability, and the availability of reliable spatial datasets for the study area. These factors collectively represent the major topographic, hydrological, environmental, and anthropogenic controls influencing landslide occurrence in the Cox's Bazar-Teknaf coastal hills. Although additional factors such as lithology, land use/land cover (LULC), Topographic Wetness Index (TWI), Stream Power Index (SPI), and lineament density have been employed in other studies, they were not included in the present analysis because of limitations in obtaining consistent, high-resolution datasets and to minimize redundancy among highly correlated variables. The selected conditioning factors provide a comprehensive representation of the dominant processes governing landslide susceptibility within the study area while maintaining model reliability and reducing uncertainty.

Elevation

Elevation plays an important role in landslide susceptibility by controlling potential energy, micro-climate, weathering, and vegetation; many studies find landslides concentrated in specific elevation bands (Chang et al., 2019; He et al., 2012).

In this study, elevation was classified into four classes ranging from 11 to 261 m. Higher elevations are mainly concentrated in the southern Teknaf hills, with elevation values ranging from 135 to 261 m. Lower elevations are primarily located in the valley between the Cox’s Bazar and Teknaf hill ranges.

Slope

Slope angle is consistently one of the most influential predictors and are top-ranked in logistic regression, jackknife and global reviews (Conforti et al., 2021; Saleem et al., 2019). Steeper slopes generally exhibit higher gravitational stress and reduced shear strength, increasing the likelihood of mass movement.

Landslide frequency typically increases with slope angle up to a threshold beyond which material availability may decrease. For this study, slope angle was classified into five classes. Extreme slope angles are mainly concentrated in the Teknaf hills and extend toward the Cox’s Bazar region, with values ranging from 25.59° to 63.95°. Higher slope angles (15.56°–25.58°) are also concentrated in the Teknaf hills, surrounding areas of extreme slope.

Aspect

Aspect affects the potential of landslides by regulating soil moisture levels, vegetation density, evapotranspiration rates, and sun radiation exposure.

Slope failure is more likely to occur on slopes that face particular directions because they can retain more moisture or weather.

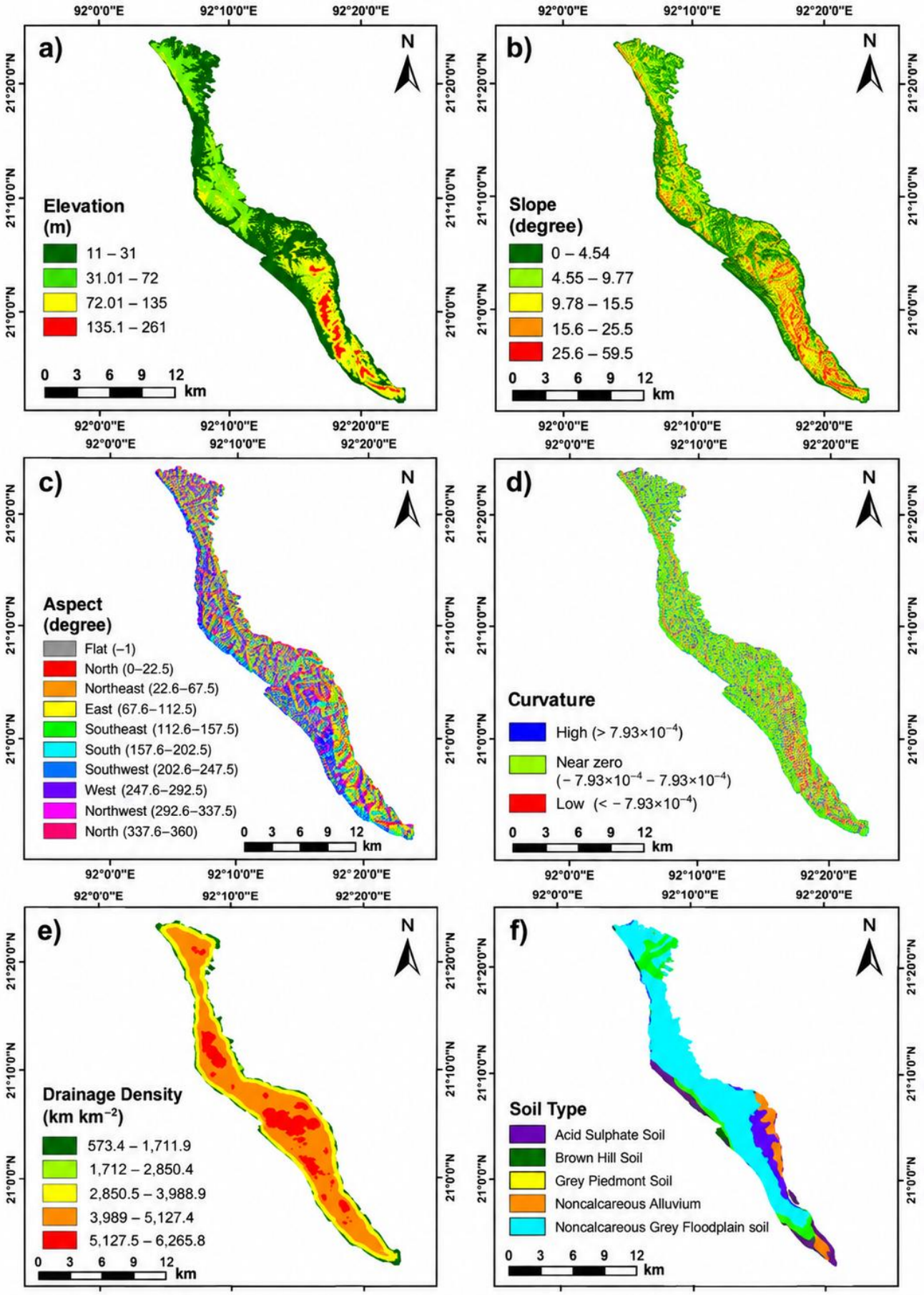


Figure 3, Landslide Conditioning Factor (a) Elevation, (b) Slope, (c) Aspect, (d) Curvature, (e) Drainage Density, (f) Soil Type

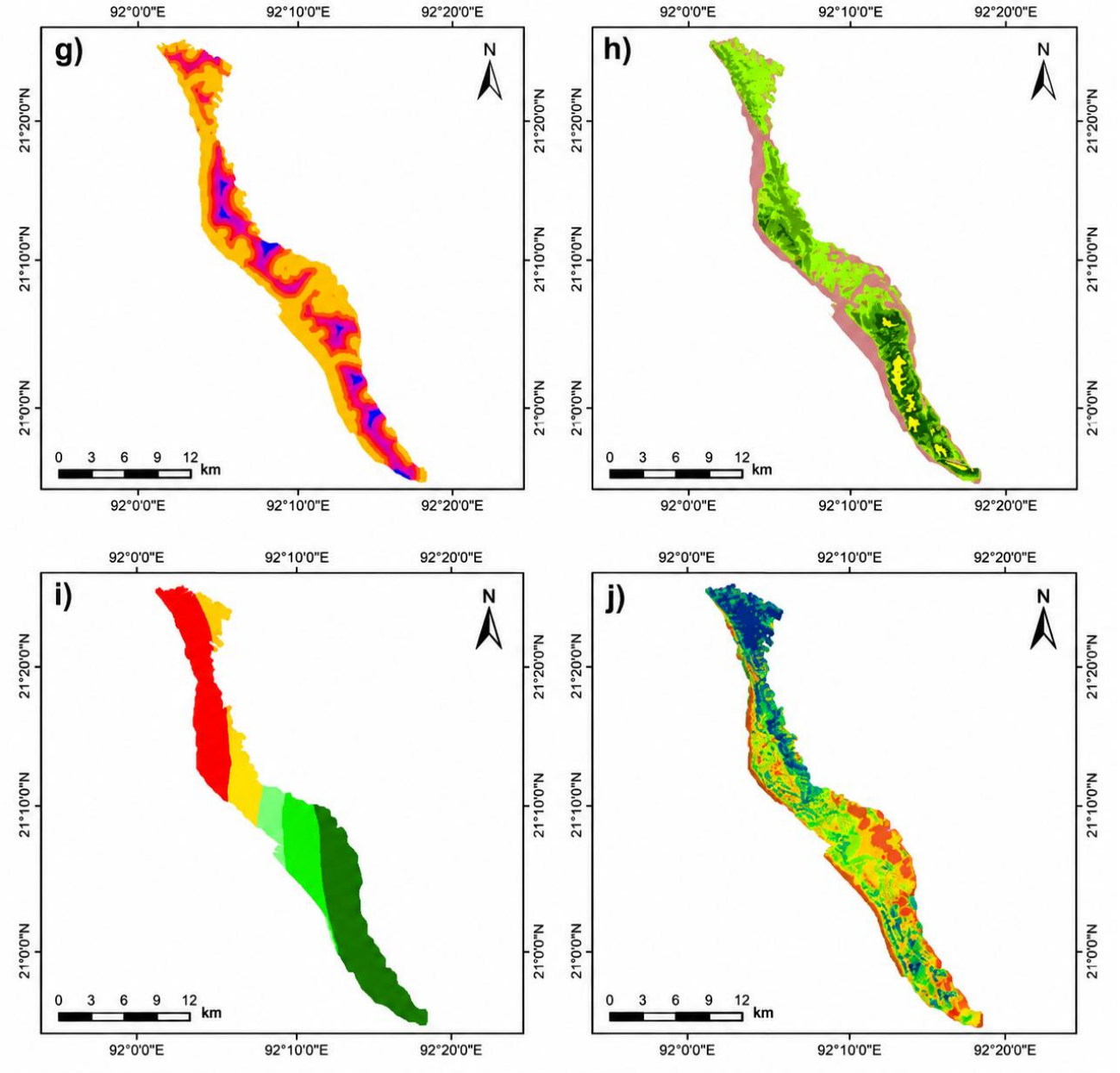


Figure 4, Landslide Conditioning Factors, contd: (g) Distance from Road, (h) Geomorphology, (i) Rainfall Map, (j) NDVI Map.

Aspect was classified into ten directional classes. Slopes facing southeast, south, and southwest are more windward and therefore receive higher monsoonal rainfall, leading to enhanced weathering, increased soil moisture, and pore-water pressure buildup, which increase landslide susceptibility. East and west facing slopes show intermediate susceptibility, whereas north-facing slopes are relatively leeward and generally exhibit lower landslide susceptibility. In parts of Cox's Bazar and Teknaf, slopes exposed to the southwest monsoon from the Bay of Bengal are particularly vulnerable to landslide occurrence.

Curvature

Curvature reflects the geometric form of the terrain and affects the convergence or divergence of surface runoff, modulating erosion and pore-pressure build-up (Huang et al., 2022). Concave slopes tend to accumulate water and sediments, increasing pore-water pressure and landslide susceptibility, whereas convex slopes generally promote runoff dispersion and exhibit comparatively lower instability. In this research, Curvature values span from approximately -1.99×10^{11} to 2.81×10^{11}, indicating alternating concave and convex surfaces across the hilly terrain.

Drainage density

Drainage density represents the degree of surface dissection by stream networks and is closely related to erosion intensity and subsurface hydrological processes. Areas with high drainage density are often characterized by intense surface runoff, channel erosion and slope undercutting which weaken Slope materials and enhance landslide susceptibility (Conforti et al., 2021). Here, Drainage density ranges from 573.4 to 6,265.8 m/km^2, with higher densities concentrated in the central and southern hill tracts where runoff channels are more frequent.

Soil type

Soil type plays a critical role in landslide susceptibility by influencing shear strength, permeability, and water-holding capacity (Moon et al., 2024). The study area is characterized by several soil types, including acid sulphate soil, brown hill soil, grey piedmont soil, noncalcareous alluvium, and noncalcareous grey floodplain soil. Brown hill soils and noncalcareous soils, which dominate the hilly and piedmont regions, are generally more prone to landslides due to their loose texture, moderate-to-high permeability, and susceptibility to saturation during intense rainfall. In contrast, floodplain and alluvial soils, predominantly distributed in low-lying areas, exhibit comparatively lower landslide susceptibility mainly due to gentler slopes and reduced gravitational driving forces.

Distance from road

Distance from road is an important anthropogenic factor influencing slope stability, as road construction often involves slope cutting, vegetation removal, and modification of natural drainage patterns (He et al., 2025). Areas closer to roads exhibit higher landslide susceptibility due to increased slope undercutting, altered runoff pathways, and reduced soil cohesion.

In the study area, distances from roads range from 0-0.023 km, highlighting zones in close proximity to major road corridors where landslide-prone areas are concentrated. Landslide susceptibility generally decreases with increasing distance from roads, reflecting reduced anthropogenic disturbance.

Geomorphology

Geomorphological units represent the surface appearance of geological structure and erosional-depositional processes, which have a significant effect on the occurrence of landslides. The study area comprises hilltops, hill slopes, lower hills, valleys, and barren land. Hill slopes and lower hill units are particularly susceptible to landslides due to steep gradients, active erosion, and weathered materials. Valleys and low-relief areas generally show lower susceptibility because of reduced slope angles and sediment accumulation, while barren lands may exhibit localized instability depending on slope conditions and surface exposure.

Rainfall

Rainfall is an important conditioning and triggering factor for landslides, especially in humid tropical and monsoon-dominated regions. It softening soils and raising pore pressure (He et al., 2025). The spatial variation in annual rainfall across the study area reflects the influence of the southwest monsoon from the Bay of Bengal, with rainfall ranging from 2399 to 2593 mm and gradually increasing from the northern belt toward the southern hilly region. Areas receiving higher rainfall experience enhanced infiltration, elevated pore-water pressure, and reduced shear strength, which collectively increase landslide susceptibility. Consequently, the southern and coastal portions of the study area, which receive relatively higher rainfall, exhibit greater vulnerability compared to regions with lower precipitation.

Normalized Difference Vegetation Index (NDVI)

Vegetation cover, represented by the Normalized Difference Vegetation Index (NDVI), plays an important role in landslide susceptibility by influencing root reinforcement, surface runoff, and soil moisture conditions (Gao et al., 2022). Low NDVI values generally indicate sparse or degraded vegetation, resulting in reduced root cohesion, greater surface exposure, and increased susceptibility to erosion and slope failure. In contrast, higher NDVI values are commonly associated with denser vegetation, which can enhance slope stability through stronger root reinforcement and reduced runoff.

In the study area, NDVI values range from −0.0573 to 0.458, reflecting spatial variation in vegetation cover. Sparse vegetation occurs mainly in the southeastern region, whereas denser vegetation is concentrated toward the northern and eastern hilly areas, including Himchari National Park.

Landslide susceptibility modeling

Analytic Hierarchy Process (AHP) based model

A structured multi-criterion decision-making (MCDM) method developed by Saaty (1977) called the Analytic Hierarchy Process (AHP) is frequently used in landslide susceptibility assessments to ascertain the relative significance of causal elements. It features a methodical framework for evaluating complicated issues involving several qualitative and quantitative criteria.

All conditioning factor layers were prepared and standardized to a common spatial resolution and coordinate system. The pairwise comparison matrix for the Analytic Hierarchy Process (AHP) was developed following Saaty's (1980) fundamental 1-9 scale (Table 2) under the guidance of a geotechnical engineering expert with extensive experience in slope stability assessment and geotechnical investigations.

The relative importance assigned to each conditioning factor was determined based on published literature, the geomorphological characteristics of the study area, and expert judgment. The preliminary weighting scheme was further reviewed through consultation with additional faculty members specializing in geology and geotechnical engineering to ensure its scientific validity and consistency. Subsequently, the pairwise comparison matrix and the corresponding weights were computed by the research team following the expert guidance, and the final matrix was verified and approved by the supervising expert.

Table 2, Saaty's Factor Ranking Scale

Importance Scores	Definition
1	Equal importance
3	Moderate importance
5	Strong importance
7	Very strong importance
9	Extreme importance
2, 4, 6, 8	Intermediate values
Reciprocals	Inverse comparison

For ensuring the accuracy of judgments, AHP employs a Consistency Ratio (CR), which rates the logical structure of the comparisons. A CR score of less than 0.10 indicates acceptable consistency, whereas greater levels suggest that judgments need to be revised. For landslide susceptibility analysis, ten factors were used as inputs. To perform the AHP calculations, pairwise comparison matrices were prepared based on the priority scale shown in Table 3.

The pairwise comparison matrix presented in Table 3 was first processed by summing the values within each column. These column totals were then used to normalize the matrix (Table 4), where each element of the original comparison matrix was divided by the sum of its respective column. This normalization step allowed the relative contribution of each factor to be expressed on a comparable scale. To derive the final weight of each landslide-conditioning factor, the average value of each row in the normalized matrix was calculated, resulting in the weights vector shown in the final column of Table 4. The results indicate that elevation received the highest weight (29%), followed by slope (21%) and soil type (15%), highlighting their dominant influence on landslide susceptibility in the study area. Distance from roads accounted for 11%, while NDVI contributed 8%. Lower weights were assigned to curvature (5%), drainage density (4%), geomorphology (3%), aspect (2%), and rainfall (2%), reflecting their comparatively smaller influence in the model. The comparatively higher weights assigned to elevation and slope are supported by expert opinion, previous studies and the geomorphological characteristics of the study area. Elevation controls terrain relief, weathering intensity, drainage development, and gravitational potential, whereas slope directly influences shear stress and slope stability, making it one of the most influential factors governing landslide occurrence. Previous studies conducted in the Chattogram Hill Tracts have consistently identified elevation and slope as the dominant conditioning factors associated with rainfall-induced landslides.

Table 3, The Pairwise Comparison Matrix and relative importance scores for Landslide susceptibility Mapping

Atributes	Elevation	Slope	Soil type	Distance from road	NDVI	Curvature	Drainage density	Geomorphology	Aspect	Rainfall
Elevation	1	2	3	4	5	6	7	8	9	9
Slope	0.5	1	2	3	4	5	6	7	8	9
Ssoil type	0.333	0.5	1	2	3	4	5	6	7	8
Distance from road	0.25	0.333	0.5	1	2	3	4	5	6	7
NDVI	0.2	0.25	0.333	0.5	1	2	3	4	5	6
Curvature	0.167	0.2	0.25	0.333	0.5	1	2	3	4	5
Drainage density	0.143	0.167	0.2	0.25	0.333	0.5	1	2	3	4
Geomorphology	0.125	0.143	0.167	0.2	0.25	0.333	0.5	1	2	3
Aspect	0.111	0.125	0.143	0.167	0.2	0.25	0.333	0.5	1	2
Rainfall	0.111	0.111	0.125	0.143	0.167	0.2	0.25	0.333	0.5	1

Table 4, The Normalization matrix and corresponding criteria weights of the landslide conditioning factors

Conditioning factors	Class											Criteria Weight
	1	2	3	4	5	6	7	8	9	10	11	
Elevation	0.340127	0.414167	0.388709	0.345040	0.303951	0.289260	0.240688	0.271795	0.197802	0.168667	0.288361	0.151769
slope	0.170063	0.207084	0.259139	0.258780	0.243161	0.224383	0.206304	0.190045	0.175824	0.168667	0.129570	0.210145
soil type	0.113376	0.103542	0.129570	0.172520	0.182371	0.179506	0.171920	0.162896	0.153846	0.148148	0.151769	0.151769
Distance from road	0.085032	0.069028	0.064785	0.086260	0.121581	0.134630	0.137536	0.135747	0.131868	0.129630	0.109609	0.109609
NDVI	0.068025	0.051771	0.043190	0.043130	0.060790	0.089753	0.103152	0.108597	0.109890	0.111111	0.078941	0.078941
Curvature	0.056688	0.041417	0.032392	0.028753	0.030395	0.044877	0.068768	0.081448	0.087912	0.092593	0.056524	0.056524
Drainage Density	0.048590	0.034514	0.025914	0.021565	0.020263	0.022438	0.034384	0.054299	0.065934	0.074074	0.040197	0.040197
Geomorphology	0.042516	0.029583	0.021595	0.017252	0.015198	0.014959	0.017192	0.027149	0.043956	0.055556	0.028496	0.028496
Aspect	0.037792	0.025885	0.018510	0.014377	0.012158	0.011219	0.011461	0.013575	0.021978	0.037037	0.020399	0.020399
Rainfall	0.037792	0.023009	0.016196	0.012323	0.010132	0.008975	0.008596	0.009050	0.010989	0.018519	0.015558	0.015558

After deriving the weight vector, the consistency of the pairwise comparisons were assessed to ensure the reliability of the expert judgments. The analysis yielded a maximum eigenvalue (λ_{max}) of 10.56, from which a Consistency Index (CI) of 0.063 was calculated. Using the corresponding Random Index (RI) value of 1.50, the Consistency Ratio (CR) was determined to be 0.042. As the CR value is well below the commonly accepted threshold of 0.10, it indicates a high level of consistency in the pairwise comparisons, confirming the reliability of the AHP-derived weights.

Therefore, the pairwise comparison matrix is considered logically consistent and suitable for application in the final landslide susceptibility assessment. Based on the derived criteria weights, the final AHP-based landslide susceptibility map was produced.

Frequency Ratio (FR) based model

The frequency ratio (FR) method is based on the fundamental assumption that future landslides are more likely to occur under environmental conditions similar to those associated with past landslide events. This approach quantifies how much more or less frequently landslides occur within each class of a conditioning factor compared to what would be expected by random chance. In this study, a landslide inventory map was prepared using historical landslide records obtained from NASA's global landslide database, complemented by visual interpretation of high-resolution imagery from Google Earth is shown in Figure 5.

This inventory served as the dependent variable in the FR analysis. The independent variables comprised ten selected landslide-conditioning factors. Each conditioning factor was classified into several thematic classes based on its spatial characteristics.

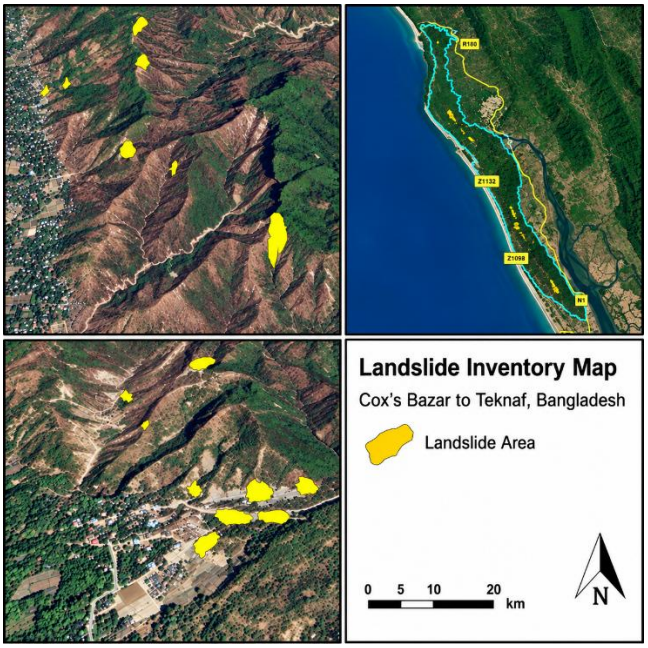


Figure 5, Landslide inventory map of the Cox's Bazar–Teknaf region, Bangladesh, showing mapped landslide locations (yellow).

The frequency ratio value for each class was calculated by dividing the percentage of landslide pixels occurring within that class by the percentage of the total study area occupied by the same class. The Frequency Ratio (FR) values were calculated using Eq. (1), and the corresponding FR calculations for all conditioning factor classes are presented in Table 5.

$$FR = \frac{\left(\frac{Number\ of\ landslide\ pixels\ in\ a\ class}{Total\ number\ of\ landslide\ pixels}\right)}{\left(\frac{Number\ of\ pixels\ in\ a\ class}{Total\ number\ of\ pixels\ in\ the\ study\ area}\right)} \quad (1)$$

The calculated Frequency Ratio (FR) values indicate the degree of association between each conditioning factor class and historical landslide occurrence. An FR value greater than 1.0 indicates that landslides occur more frequently than expected within a particular class

and therefore exhibit a positive relationship with landslide susceptibility, whereas FR values less than 1.0 indicate comparatively lower susceptibility. The results demonstrate that higher elevation and steeper slope classes generally exhibit higher FR values, confirming their dominant influence on landslide occurrence. Likewise, higher FR values associated with areas of sparse vegetation, shorter distances from roads, and specific geomorphological units highlight the combined influence of topographic, environmental, and anthropogenic factors on slope instability.

These FR values were subsequently used to assign class weights for the preparation of the FR-based landslide susceptibility map.

After preparation of the landslide-conditioning factor layers, all datasets were converted to raster format and standardized to a common spatial resolution, projection, and spatial extent to ensure consistency. Each conditioning factor was reclassified into susceptibility classes using the Reclassify tool in ArcGIS 10.8, based on its relative contribution to landslide occurrence as determined by the applied susceptibility models (Addis, 2023).

Landslide susceptibility mapping was carried out using a raster-based weighted overlay approach implemented through the Raster Calculator tool within the Spatial Analyst extension of ArcGIS 10.8. In this process, each reclassified factor raster was multiplied by its corresponding weight, and the weighted raster were summed to generate the Landslide Susceptibility Index (LSI), by the following equation 2 (Pradhan, 2010).

$$LSI = \Sigma(Wi \times Ri) \qquad (2)$$

Where, Wi denotes the weight assigned to the i^{th} conditioning factor and Ri represents its reclassified raster value.

The generated Landslide Susceptibility Index (LSI) raster effectively captures the spatial variability of landslide susceptibility across the study area, highlighting zones with differing levels of potential landslide occurrence (Rasyid et al., 2016). Higher LSI values represent areas with greater susceptibility, whereas lower values indicate comparatively stable regions. To produce the final landslide susceptibility map, the continuous LSI values were classified using the Natural Breaks (Jenks) classification method. This approach groups values by minimizing within-class variance and maximizing between-class differences, allowing for an objective delineation of susceptibility patterns. The classified map was divided into five susceptibilities zones- very low, low, moderate, high, and very high to clearly represent the spatial distribution of landslide-prone areas and support effective hazard assessment and land-use planning.

Model validation

The predictive performance of the landslide susceptibility maps produced using the Analytic Hierarchy Process (AHP) and Frequency Ratio (FR) models was evaluated through a standard model validation procedure based on the Receiver Operating Characteristic (ROC) curve and the Area under the Curve (AUC) (Panchal & Shrivastava, 2021; Ali et al., 2025). Validation was carried out using the landslide inventory dataset, which represents the observed spatial distribution of past landslide events within the study area (Wang et al., 2017).

The ROC-AUC approach is a threshold-independent statistical method widely used to assess the reliability and robustness of susceptibility models. It measures the ability of a model to correctly distinguish between landslide-prone and non-landslide areas across a range of classification thresholds (Chen et al., 2019; Ali et al., 2025). In this study, the ROC curves were generated using Python 2.7.16 with the Scikit-learn, Pandas, NumPy, and Matplotlib libraries by comparing the landslide susceptibility values at the inventoried landslide locations with those at the non-landslide locations. Model performance was evaluated using a validation dataset consisting of 55 landslide points and 30 non-landslide points. The true positive rate (landslide locations) and false positive rate (non-landslide locations) were calculated across a range of threshold values to construct the ROC curves and determine the Area Under the Curve (AUC).

The AUC value, which ranges from 0.5 to 1.0, provides a quantitative measure of model accuracy (Dahal et al., 2008a; Dahal et al., 2008b; Chen et al., 2019; Kusuma et al., 2025). An AUC value close to 1.0 indicates excellent predictive capability, while values near 0.5 suggest random prediction. Generally, AUC values between 0.9-1.0 represent very high accuracy, 0.8-0.9 indicate good performance, 0.7-0.8 reflect moderate accuracy, and values below 0.7 imply poor classification. Conditioning factors with AUC values greater than 0.6 are considered to have a meaningful contribution to landslide occurrence (Kusuma et al., 2025).

The ROC curves and corresponding AUC values demonstrate that both the AHP and FR models perform well in capturing the spatial relationship between landslide occurrences and controlling factors. A higher AUC value indicates stronger agreement between predicted susceptibility classes and observed landslide locations, confirming the reliability of the developed landslide susceptibility maps for hazard assessment and planning purposes (Wubalem, 2020).

Result and discussion

The assessment of landslide susceptibility in the study area was conducted using two distinct modeling approaches, the knowledge-based Analytic Hierarchy Process (AHP) and the data-driven Frequency Ratio (FR) model illustrated in Figure 6.

AHP-based results show that the study area is predominantly classified as moderate susceptible, accounting for about 63.48% of the total area, followed by low susceptibility (35.45%) and a very limited high-susceptibility zone (1.06%). Spatially, high- susceptible areas are mainly concentrated along the southeastern hill slopes of Teknaf, where steep slopes and geomorphic instability prevail. Moderate-susceptible zones extend widely across Ramu, Ukhiya, and Teknaf Upazila, reflecting transitional terrain conditions. In contrast, low- susceptible areas are largely distributed over the coastal plains and relatively flat regions, where slope instability potential is minimal.

Table 5, Frequency Ratio (FR) calculation for the conditioning factor classes used in landslide susceptibility assessment.

Parameter	Classes	Class Pixels	%Class Pixels	Landslide Pixels	%Landslide Pixels	FR	RF	RF (non%)	RF (INT)	Min RF	Max RF	Max-Min RF	(Max-Min)/ Min RF	PR
Slope	0 – 4.514	128613	39.903	1.000	3.125	0.0000	0.003	0.284817	0					
	4.515 – 9.279	100762	31.262	9.000	28.125	0.0001	0.033	3.271872	3					
	9.28 – 15.55	60202	18.678	4.000	12.500	0.0001	0.024	2.433883	2					
	15.56 – 25.58	27286	8.466	5.000	15.625	0.0002	0.067	6.712445	6					
	25.59 – 63.95	5455	1.692	13.000	40.625	0.0024	0.873	87.29698	87					
	Total	**322318**		32.000		0.0027				0.002848	0.87297	0.870122	0.202983	4.286667
Elevation	(-)11 – 24	125628	38.389	1.000	3.125	0.0000	0.005	0.454787	0					
	24.01 – 50	119221	36.432	7.000	21.875	0.0001	0.034	3.354591	3					
	50.01 – 90	52131	15.930	4.000	12.500	0.0001	0.044	4.383875	4					
	90.01 – 149	20917	6.392	9.000	28.125	0.0004	0.246	24.58314	24					
	149.1 – 261	9349	2.857	11.000	34.375	0.0012	0.672	67.22361	67					
	Total	**327246**			32.000	0.0018				0.004548	0.672236	0.667688	0.202983	3.289376
Soil Type	Acid Sulphate Soil	24707	8.470	1.000	3.226	0.0000	0.046	4.596086	4					
	Brown Hill Soil	31277	10.722	5.000	16.129	0.0002	0.182	18.15319	18					
	Grey Piedmont Soil	17290	5.927	6.000	19.355	0.0003	0.394	39.40619	39					
	Noncalcareous Aluvium	22478	7.706	6.000	19.355	0.0003	0.303	30.3111	30					
	Noncalcareous Grey Floodplain soil	195956	67.175	13.000	41.935	0.0001	0.075	7.533433	7					
	Total	291708			31.000	0.0009				0.046	0.394062	0.3481	0.202983	1.714925
Geomorphology	Baren land	124286	53.390	4.000	12.500	0.0000	0.021	2.128362	2					
	Hill Slopes	69453	29.835	8.000	25.000	0.0001	0.148	14.81715	14					
	Hilltops	26779	11.503	6.000	18.750	0.0002	0.076	7.617398	7					
	Valleys	12273	5.272	14.000	43.750	0.0011	0.754	75.43709	75					
	Total	232791			32.000	0.0015				0.021284	0.754371	0.733087	0.202983	3.611565
Rainfall	2,399 – 2,437	91026	45.954	6.000	18.750	0.0001	0.213	21.34692	21					
	2,555 – 2,593	107055	54.046	26.000	81.250	0.0002	0.787	78.65308	78					
	Total	198081			32.000	0.0003				0.213469	0.786531	0.573062	0.202983	2.823197
Drainage Density	1,712 – 2,850.4	48953	16.690	3.000	9.375	0.0001	0.185	18.45309	18					
	2,850.5 – 3,988.9	70143	23.915	1.000	3.125	0.0000	0.043	4.29282	4					
	3,989 – 5,127.4	117487	40.057	26.000	81.250	0.0002	0.666	66.63626	66					
	5,127.5 – 6,265.8	56718	19.338	2.000	6.250	0.0000	0.106	10.61784	10					
	Total	293301			32.000	0.0003				0.042928	0.666363	0.623434	0.202983	3.071358
Distance From Road	0 – 0.00459	116236	35.494	2.000	6.250	0.0000	0.028	2.806812	2					
	0.0046 – 0.00918	80036	24.440	5.000	15.625	0.0001	0.102	10.19081	10					
	0.00919 – 0.0138	63798	19.481	10.000	31.250	0.0002	0.256	25.56919	25					
	0.0139 – 0.0184	45692	13.953	13.000	40.625	0.0003	0.464	46.41167	46					
	0.0185 – 0.023	21719	6.632	2.000	6.250	0.0001	0.150	15.02153	15					
	Total	327481			32.000	0.0006				0.028068	0.464117	0.436049	0.202983	2.148199
NDVI	(-)0.0573 – 0.106	37867	11.573	3.000	9.375	0.0001	0.159	15.94784	15					
	0.107 – 0.169	80503	24.604	10.000	31.250	0.0001	0.250	25.00515	25					
	0.17 – 0.223	98303	30.044	5.000	15.625	0.0001	0.102	10.2387	10					
	0.224 – 0.286	60130	18.377	11.000	34.375	0.0002	0.368	36.82503	36					
	0.287 – 0.458	50395	15.402	3.000	9.375	0.0001	0.120	11.98327	11					
	Total	327198			32.000	0.0005				0.102387	0.36825	0.265863	0.202983	1.309779
Aspect	Flat (-1)	39127	13.653	1.000	3.125	0.0000	0.029	2.891633	2					
	North (0–22.5)	35523	12.395	4.000	12.500	0.0001	0.127	12.74002	12					
	Northeast (22.5–67.5)	35782	12.486	7.000	21.875	0.0002	0.221	22.13365	22					
	Southeast (112.5–157.5)	36406	12.704	3.000	9.375	0.0001	0.093	9.323263	9					
	South (157.5–202.5)	39031	13.620	8.000	25.000	0.0002	0.232	23.18996	23					
	Southwest (202.5–247.5)	37953	13.243	4.000	12.500	0.0001	0.119	11.92432	11					
	West (247.5–292.5)	32074	11.192	4.000	12.500	0.0001	0.141	14.10998	14					
	Northwest (292.5–337.5)	30685	10.707	1.000	3.125	0.0000	0.037	3.687173	3					
	Total	286581			32.000	0.0009				0.028916	0.2319	0.202983	0.202983	1
Curvature	High	121622	37.166	19.000	59.375	0.0002	0.547927	54.79267	54					
	Moderate	113603	34.716	6.000	18.750	0.0001	0.185243	18.52433	18					
	Low	92012	28.118	7.000	21.875	0.0001	0.26683	26.683	26					
	Total	327237			32.000	0.0003				0.185243	0.547927	0.362683	0.202983	1.786765

In comparison, the FR-based model provides a more detailed zonation by dividing the area into five susceptibility classes. The results indicate dominance of very low susceptibility (44.75%) and low susceptibility (38.39%) zones, together covering more than 80% of the study area. Moderate- susceptibility areas (12.51%) appear as scattered patches, mainly within the hill tracts of Teknaf and parts of Ukhiya.

Importantly, the FR model identifies high-susceptibility (3.91%) and very high-susceptibility (0.44%) zones, which form distinct and continuous clusters along the steep southeastern slopes of Teknaf,

highlighting zones of pronounced terrain instability. A comparison of spatial extent reveals notable differences between the two models. The AHP model allocates a larger proportion of land to the moderate-susceptibility category, suggesting a more generalized classification. In contrast, the FR model concentrates most of the area within very low and low- susceptibility classes, while simultaneously identifying a higher combined percentage of high and very high-Susceptibility zones (4.35%). This indicates that the FR approach is more sensitive in distinguishing unstable terrain and capturing localized high- susceptible areas.

Area-based analysis further supports this distinction. While AHP assigns only 2.73 km^2 to the high-susceptibility category, the FR model identifies approximately 11.14 km^2 as high to very high susceptibility combined shown in Table 6. The differences in the spatial patterns of the AHP and FR models arise from their methodological approaches.

The AHP model produces more generalized susceptibility patterns based on expert-assigned weights, whereas the FR model identifies more localized high-susceptibility zones by statistically relating historical landslides to conditioning factor classes.

The ROC-AUC validation results demonstrate clear differences in predictive capability between the two models in Figure 7. The AHP model achieved an AUC value of 0.859, indicating strong predictive performance and a high level of agreement between predicted susceptibility and observed landslide locations. Conversely, the FR model yielded an AUC value of 0.688, representing moderate predictive capability.

The susceptibility patterns identified in the present study are generally consistent with previous landslide susceptibility investigations conducted in the Chattogram Hill Tracts and southeastern Bangladesh, where elevation, slope, rainfall, and anthropogenic activities have been recognized as the dominant controls on slope instability (Sultana et al., 2024; Islam et al., 2024; Nahar et al., 2025). Similar studies employing AHP, Frequency Ratio, and other GIS-based approaches have likewise reported that steep hill slopes, higher elevations, and road-cutting activities significantly increase landslide susceptibility (Chowdhury et al., 2023; Rabby and Li, 2020). The concentration of high and very high susceptibility zones in the Teknaf and Ukhiya hill regions observed in this study therefore agrees well with earlier investigations, confirming the strong influence of both geomorphological conditions and human-induced landscape modifications. The higher predictive performance of the AHP model also supports previous findings that expert knowledge can effectively represent complex terrain characteristics in data-limited environments, whereas the FR model provides greater spatial detail by directly incorporating the statistical relationship between historical landslide occurrences and conditioning factors.

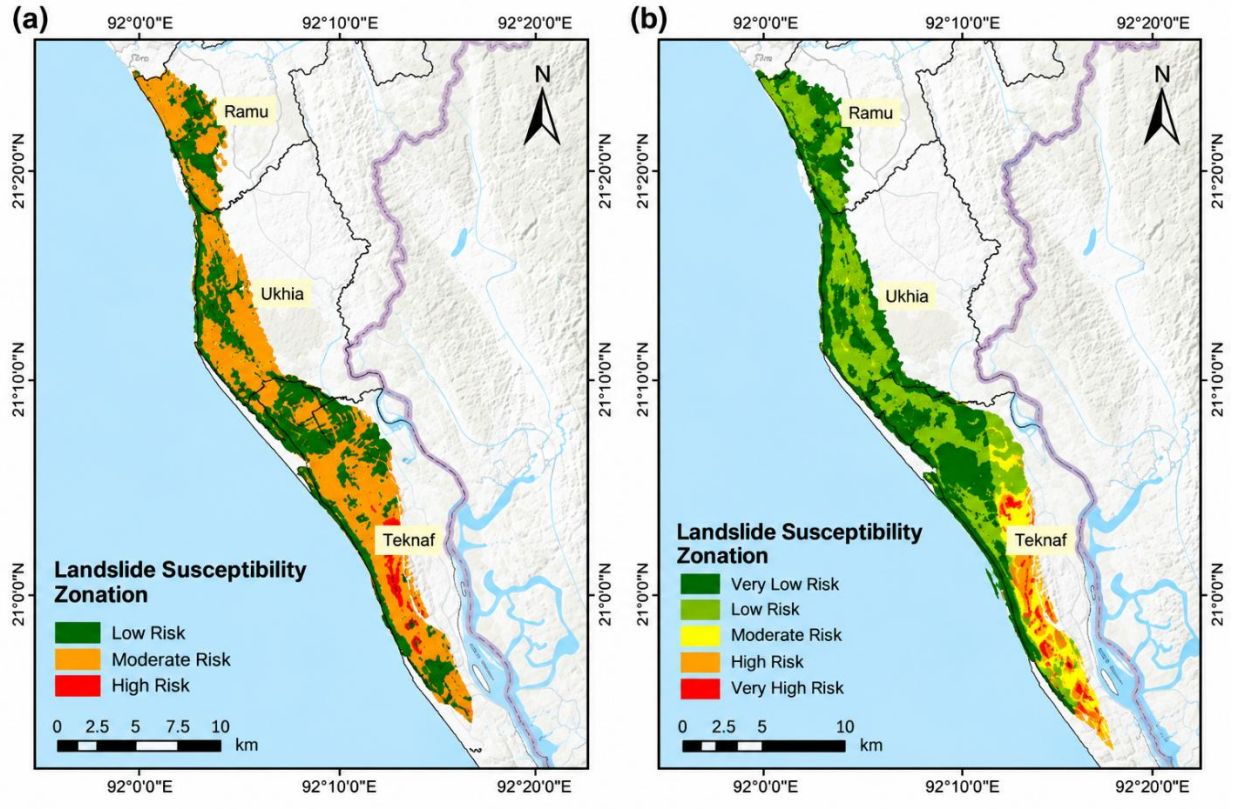


Figure 6, Landslide Susceptibility mapping of the study area, (a) AHP based susceptibility mapping and (b) FR based susceptibility mapping.

The generated landslide susceptibility maps and identified high- and very high-susceptibility zones can assist government agencies and local authorities in prioritizing slope stabilization, regulating hill-cutting activities, and guiding infrastructure development in vulnerable areas. The maps also provide valuable information for emergency preparedness, land-use planning, and humanitarian management, particularly in the Ukhiya–Teknaf corridor where transportation infrastructure, settlements, and refugee camps are exposed to recurrent landslide hazards.

Table 6, Spatial Extent of Susceptibility Class in AHP and FR Models

AHP Based Model		
Susceptibility Class	**Area (Km²)**	**Percentage (%)**
Low	90.87	35.45
Moderate	162.72	63.48
High	2.73	1.06
FR Model		
Susceptibility Class	**Area (Km²)**	**Percentage (%)**
Very Low	114.62	44.75
Low	98.33	38.39
Moderate	32.04	12.51
High	10.03	3.91
Very High	1.11	0.44

Despite these encouraging results, the present study relied primarily on ROC-AUC analysis for model validation. Although ROC-AUC is a robust and widely accepted metric for evaluating landslide susceptibility models, incorporating additional validation measures, such as confusion matrix-based indices (e.g., precision, recall, F1-score, and overall accuracy), the Kappa coefficient, and Success Rate Curves, would provide a more comprehensive assessment of model performance and predictive reliability.

Limitations and future research

This study has several limitations that should be considered when interpreting the results. The landslide inventory was compiled from the NASA Global Landslide Catalog and Google Earth imagery; therefore, some undocumented landslide events may not have been captured. In addition, the input datasets differ in source, spatial resolution, and acquisition time, introducing unavoidable uncertainties. The AHP model relies on expert judgment, whereas the FR model assumes that future landslide occurrence follows historical spatial patterns. The pairwise comparison matrix satisfied the recommended consistency criterion (CR < 0.10); however, a formal sensitivity analysis was not performed. Furthermore, the susceptibility maps represent the relative likelihood of landslide occurrence rather than deterministic predictions. Despite these limitations, the ROC-AUC validation (Figure 7) results indicate that the models provide a reliable basis for regional landslide hazard assessment. Future research should incorporate sensitivity analysis, field-based validation, higher-resolution datasets, and additional statistical and machine-learning approaches, such as Logistic Regression (LR), Random Forest (RF), Support Vector Machine (SVM), and Extreme Gradient Boosting (XGBoost), to further improve model robustness and predictive performance. In addition, future studies should include systematic field investigations and independent validation datasets to verify the identified susceptibility zones and further improve the reliability of landslide susceptibility assessments.

Conclusion and recommendations

This study applied AHP and FR-based landslide susceptibility models to identify and compare spatial patterns of landslide susceptibility in the study area. The findings demonstrate the effectiveness of integrating expert-based and data-driven approaches to identify landslide-prone areas and provide a scientifically reliable framework for regional hazard assessment. The generated susceptibility maps contribute valuable spatial information to support evidence-based planning, infrastructure development, and disaster risk management in one of Bangladesh's most landslide-prone regions. The complementary performance of these models demonstrates that their combined application can improve landslide susceptibility assessment by integrating expert knowledge with statistically derived spatial relationships.

Based on the findings, the following recommendations are proposed to support risk reduction and sustainable land management.

1. Risk-sensitive land-use planning

High and very high landslide susceptibility zones, especially along the steep slopes of Teknaf, should be strictly regulated. New settlements, road construction, and slope cutting activities should be avoided or minimized in these areas.

2. Rohingya refugee camp management

Several refugee camps are located in or adjacent to moderate- to high-susceptibility zones. Immediate attention should be given to relocating shelters away from high-risk slopes, enforcing slope setbacks, and limiting hill cutting for fuelwood or shelter expansion. Temporary stabilization measures, such as surface drainage control and bioengineering techniques, should be implemented where relocation is not immediately feasible.

3. Slope stabilization along marine drive and coastal cliffs

The marine drive corridor, which runs along steep coastal cliffs, is highly vulnerable to slope failure due to combined effects of steep gradients, rainfall, and

coastal erosion. Regular geotechnical inspections, controlled drainage systems, retaining structures, and vegetation-based slope reinforcement are strongly recommended to reduce landslide risk and ensure road safety.

4. Integrated use of susceptibility models

For practical applications, it is recommended to use AHP for regional-scale planning and FR for site-specific risk identification, as their combined application provides a more comprehensive understanding of landslide susceptibility.

Overall, the results of this study provide a valuable scientific basis for disaster risk reduction strategies, infrastructure planning, and humanitarian management in a highly vulnerable and socio-environmentally sensitive region.

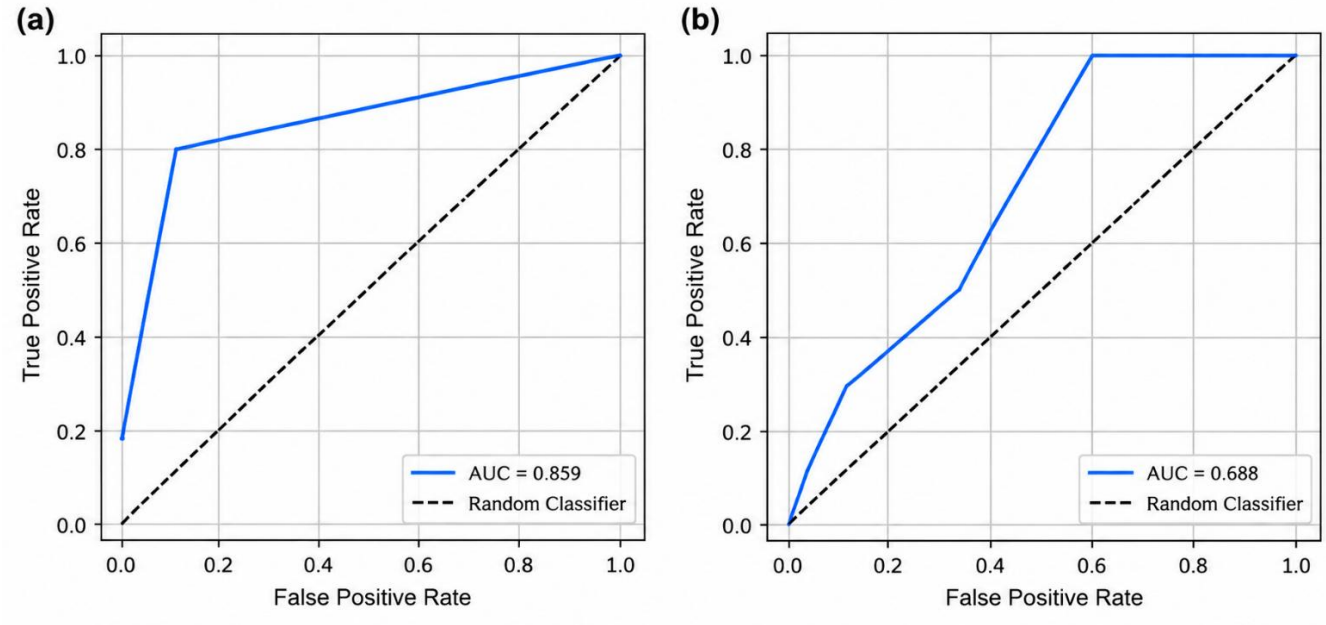


Figure 7, ROC–AUC curves of the (a) AHP and (b) FR landslide susceptibility models.

Acknowledgements

Special thanks to Prof. Dr. Younus Ahmed Khan for his insightful ideas and academic support. The author further thanks the IAEG YEG, University of Rajshahi (UR), Bangladesh team for fostering an enthusiastic research environment and creating a festive academic spirit during the 15th ARC Conference.

Author contributions

Muqit Ajmain Shahriyar conceived the research idea, conducted data analysis, prepared the figures, and wrote the original manuscript. Dr. Md. Abdul Malek supervised the study and provided continuous guidance in structuring the research framework and methodology.

Md. Yunus Hider, Tasmim Banu, and Md. Mahedi Hasan contributed to manuscript writing, critical revision, and overall improvement of the paper. Tasmim Banu also presented the research at the 15th ARC Conference, Nepal. All authors reviewed and approved the final version of the manuscript.

Data availability

The data used in this study are not publicly available. The datasets and analytical outputs generated during the study are available from the corresponding author upon reasonable request.

Declarations

The authors declare that they have no known competing financial interests or personal relationships that could have influenced the work reported in this article.

Article note

This article is a full-length paper developed from **Extended Abstract #091**, entitled "**Integrating AHP and Remote Sensing Method for Landslide Susceptibility Mapping of the Coastal Cliffs in Southeastern Bangladesh**" which was presented at the 15th Asian Regional Conference of the International Association for Engineering Geology and the Environment (ARC-15 of **IAEG**), held in Kathmandu, Nepal, from 27 to 29 November 2025.

Reference

Addis, A. (2023). GIS-Based Landslide Susceptibility Mapping Using Frequency Ratio and Shannon Entropy Models in Dejen District, Northwestern Ethiopia. Journal of Engineering. https://doi.org/10.1155/2023/1062388

Ahmed, B., Rahman, M., Sammonds, P., Islam, R., and Uddin, K. (2020). Application of geospatial technologies in developing a dynamic landslide early warning system in a humanitarian context: the Rohingya refugee crisis in Cox's Bazar, Bangladesh. Geomatics, Natural Hazards and Risk, 11, 446 - 468. https://doi.org/10.1080/19475705.2020.1730988

Ali, A., Teku, D., Sisay, T., and Mihret, B. (2025). A combined analysis of frequency ratio and analytical hierarchy process for landslide susceptibility assessment in Tenta, South Wollo, Ethiopia. Scientific Reports, 15. https://doi.org/10.1038/s41598-025-94611-z

Carrara, A. (1983). Multivariate models for landslide hazard evaluation. Journal of the International Association for Mathematical Geology, 15, 403-426. https://doi.org/10.1007/bf01031290

Chang, K., Merghadi, A., Yunus, A., Pham, B., and Dou, J. (2019). Evaluating scale effects of topographic variables in landslide susceptibility models using GIS-based machine learning techniques. Scientific Reports, 9. https://doi.org/10.1038/s41598-019-48773-2

Chen, W., Sun, Z., and Han, J. (2019). Landslide Susceptibility Modeling Using Integrated Ensemble Weights of Evidence with Logistic Regression and Random Forest Models. Applied Sciences, 9(1), 171. https://doi.org/10.3390/app9010171

Chowdhury, M. (2024). Morphometric analysis of Halda River basin, Bangladesh, using GIS and remote sensing techniques. Heliyon, 10. https://doi.org/10.1016/j.heliyon.2024.e29085

Chowdhury, M., Rahman, M., Sheikh, M., Sayeid, M., Mahmud, K., and Hafsa, B. (2023). GIS-based landslide susceptibility mapping using logistic regression, random forest and decision and regression tree models in Chattogram District, Bangladesh. Heliyon,10. https://doi.org/10.1016/j.heliyon.2023.e23424

Conforti, M., and Ietto, F. (2021). Modeling Shallow Landslide Susceptibility and Assessment of the Relative Importance of Predisposing Factors, through a GIS-Based Statistical Analysis. Geosciences, 11(8), 333. https://doi.org/10.3390/geosciences11080333.

Cuomo, S. (2020). Modelling of flowslides and debris avalanches in natural and engineered slopes: a review. Geoenvironmental Disasters, 7, 1-25. https://doi.org/10.1186/s40677-019-0133-9

Dahal, R. K., Hasegawa, S., Nonomura, A., Yamanaka, M., Masuda, T., and Nishino, K. (2008a). GIS-based weights-of-evidence modelling of rainfall-induced landslides in small catchments for landslide susceptibility mapping. Environmental Geology, 54(2), 311–324. https://doi.org/10.1007/s00254-007-0818-3

Dahal, R. K., Hasegawa, S., Nonomura, A., Yamanaka, M., Dhakal, S., and Paudyal, P. (2008b). Predictive modelling of rainfall-induced landslide hazard in the Lesser Himalaya of Nepal based on weights-of-evidence. Geomorphology, 102(3–4), 496–510. https://doi.org/10.1016/j.geomorph.2008.05.041

Fidan, S., Tanyaş, H., Akbaş, A., Lombardo, L., Petley, D.N., and Görüm, T. (2024). Understanding fatal landslides at global scales: a summary of topographic, climatic, and anthropogenic perspectives. Natural Hazards, 120, 6437 - 6455. https://doi.org/10.1007/s11069-024-06487-3

Froude, M.J., and Petley, D. (2018). Global fatal landslide occurrence from 2004 to 2016. Natural Hazards and Earth System Sciences, 18, 2161-2181. https://doi.org/10.5194/nhess-18-2161-2018

Fuad, N., Meandad, J., Haque, A., Sultana, R., Anwar, S., and Sultana, S. (2024). Landslide vulnerability analysis using frequency ratio (FR) model: a study on Bandarban district, Bangladesh. ArXiv, abs/2407.20239. https://doi.org/10.48550/arxiv.2407.20239

Gao, J., Shi, X., Li, L., Zhou, Z., and Wang, J. (2022). Assessment of Landslide Susceptibility Using Different Machine Learning Methods in Longnan City, China. Sustainability, 14(24), 16716. https://doi.org/10.3390/su142416716

He, Q., Wu, S., Zhao, X., Hui, Z., Wang, Z., Tsangaratos, P., Ilia, I., Chen, W., Chen, Y., and Hao, Y. (2025). Evaluation of landslide susceptibility of mountain highway based on RF and SVM models. Scientific Reports, 15. https://doi.org/10.1038/s41598-025-08774-w

He, S., Pan, P., Dai, L., Wang, H., & Liu, J. (2012). Application of kernel-based Fisher discriminant analysis to map landslide susceptibility in the Qinggan River delta, Three Gorges, China. Geomorphology, 171, 30-41. https://doi.org/10.1016/j.geomorph.2012.04.024

Hossain, F., and Moniruzzaman, D. M. (2021). Environmental change detection through remote sensing technique: A study of Rohingya refugee camp area (Ukhiya and Teknaf sub-district), Cox's Bazar, Bangladesh. Environmental Challenges,100024. https://doi.org/10.1016/j.envc.2021.100024

Hossain, S., Tushar, M., Islam, S., Razzak, M., Alve, A., and Junayed, T. (2025). Investigating the role of rock weathering and clay mineralogy in landslide occurrences within the exposed Tertiary Formations in Rangamati area. Geoenvironmental Disasters, 12. https://doi.org/10.1186/s40677-025-00324-w

Hossen, S., Hossain, M., Hossain, M., and Uddin, M. (2020). Quantitative assessment of tree species diversity of Himchari National Park (HNP) in Cox's Bazar, Bangladesh. Asian Journal of Forestry, 5(1), 1-7. https://doi.org/10.13057/asianjfor/r050101

Huang, F., Tao, S., Li, D., Lian, Z., Catani, F., Huang, J., Li, K., and Zhang, C. (2022). Landslide Susceptibility Prediction Considering Neighborhood Characteristics of Landslide Spatial Datasets and Hydrological Slope Units Using Remote Sensing and GIS Technologies. Remote. Sens., 14(18), 4436. https://doi.org/10.3390/rs14184436

Islam, M. T., Sikder, S. K., Charlesworth, M., and Rabbi, A. (2023). Spatial transition dynamics of urbanization and Rohingya refugees' settlements in Bangladesh. Land Use Policy, 133, 106874. https://doi.org/10.1016/j.landusepol.2023.106874

Islam, S., Miah, M., Jubaer, A., Mondal, K., and Mahmud, M. (2024). An Assessment of the Causes and Consequences of Landslides (2017) Occurred in the Southeastern Areas of Bangladesh. Journal of Science and Technology Research, 5(1). https://doi.org/10.3329/jscitr.v5i1.74011

Kamal, A., Hossain, F., Ahmed, B., Rahman, M., and Sammonds, P. (2023). Assessing the effectiveness of landslide slope stability by analysing structural mitigation measures and community risk perception. Natural Hazards, 117, 2393 - 2418. https://doi.org/10.1007/s11069-023-05947-6

Kamal, A., Hossain, F., Rahman, M., Ahmed, B., and Sammonds, P. (2022). Geological and soil engineering properties of shallow landslides occurring in the Kutupalong Rohingya Camp in Cox's Bazar, Bangladesh. Landslides, 19, 465-478. https://doi.org/10.1007/s10346-021-01810-6

Khanam, F., Rahman, M., Alam, M., and Abdullah, R. (2020). Sedimentology and basin-fill history of the Cenozoic succession of the Sylhet Trough, Bengal Basin, Bangladesh. International Journal of Earth Sciences, 110, 193-212. https://doi.org/10.1007/s00531-020-01946-1

Kusuma, R., Meilano, I., and Fitri, I. (2025). Landslide Susceptibility Assessment using Analytical Hierarchy Process in West Java. IOP Conference Series: Earth and Environmental Science, 1472, 1-13. https://doi.org/10.1088/1755-1315/1472/1/012035

Lee, S., and Pradhan, B. (2006). Probabilistic landslide hazards and risk mapping on Penang Island, Malaysia. Journal of Earth System Science, 115(6), 661-672. https://doi.org/10.1007/s12040-006-0004-0

Luna, L., Woodard, J., Bytheway, J., Belair, G., and Mirus, B. (2025). Constraining landslide frequency across the United States to inform county-level risk reduction. Natural Hazards and Earth System Sciences, 25, 3279–3304. https://doi.org/10.5194/nhess-25-3279-2025

Mazumder, A., Sarkar, A., Sikder, M., Tabassum, A., Islam, S. T., and Barua, E. (2024). Impact of Land Conversion on Land Surface Temperature Over the Coastal Area: A Spatiotemporal Study of Cox's Bazar District, Bangladesh. Journal of Geovisualization and Spatial Analysis, 8, 38. https://doi.org/10.1007/s41651-024-00196-y

Mohiuddin, M., Hossain, M., Islam, M. Y., Nowreen, S., and Sultana, N. (2025). Assessing the impact of Land Use Land Cover change after Rohingya forced migration on elephant route in Cox's Bazar district, Bangladesh. Landscape and Ecological Engineering, 21, 303 - 319. https://doi.org/10.1007/s11355-025-00642-z

Moon, S., Noh, J., Kim, H., Kang, S., and Seo, Y. (2024). Comparison of factors influencing landslide risk near a forest road in Chungju-si, South Korea. Geoenvironmental Disasters, 11, 1-17. https://doi.org/10.1186/s40677-024-00267-8

Moslehuddin, A., Rahman, M., Moriyama, M., and Tani, M. (2018). Physiography, Forests, and People in Teknaf. , 11-40. https://doi.org/10.1007/978-981-10-5475-4_2

Nahar, N., Mohiuddin, M., Nowreen, S., and Hossain, M. (2025). Influential Factors of Landslide Occurrence in the South-Eastern Part of Bangladesh. IDRiM Journal. https://doi.org/10.5595/001c.143100

Nath, T., Aziz, N., and Inoue, M. (2015). Contribution of Homestead Forests to Rural Economy and Climate Change Mitigation: A Study from the Ecologically Critical Area of Cox's Bazar—Teknaf Peninsula, Bangladesh. Small-scale Forestry, 14, 1-18. https://doi.org/10.1007/s11842-014-9270-x

Panchal, S., and Shrivastava, A. (2021). A Comparative Study of Frequency Ratio, Shannon's Entropy and Analytic Hierarchy Process (AHP) Models for Landslide Susceptibility Assessment. ISPRS Int. J. Geo Inf., 10, 603. https://doi.org/10.3390/ijgi10090603

Petley, D., Bulmer, M., and Murphy, W. (2002). Patterns of movement in rotational and translational landslides. Geology, 30, 719-722. https://doi.org/10.1130/0091-7613(2002)030<0719:pomira>2.0.co;2

Pradhan, B., and Lee, S. (2010). Delineation of landslide hazard areas using frequency ratio, logistic regression and artificial neural network models. https://doi.org/10.1007/s12665-009-0245-8

Prancevic, J., Lamb, M., McArdell, B., Rickli, C., and Kirchner, J. (2020). Decreasing Landslide Erosion on Steeper Slopes in Soil-Mantled Landscapes. Geophysical Research Letters, 47. https://doi.org/10.1029/2020gl087505

Rabby, Y., and Li, Y. (2020). Landslide Susceptibility Mapping Using Integrated Methods: A Case Study in the Chittagong Hilly Areas, Bangladesh. Geosciences. https://doi.org/10.3390/geosciences10120483

Rahman, H., and Khan, Y. A. (1995). Landslides and stability of coastal cliffs of Cox's Bazar area, Bangladesh. Natural hazards, 12(2), 101-118.

Rasyid, A., Bhandary, N., and Yatabe, R. (2016). Performance of frequency ratio and logistic regression model in creating GIS based landslides susceptibility map at Lompobattang Mountain, Indonesia. Geoenvironmental Disasters, 3, 1-16. https://doi.org/10.1186/s40677-016-0053-x

Rudra, A., and Alam, A. (2023). Streamflow characteristics of Sangu-Matamuhuri watershed in the southeastern part of Bangladesh. Heliyon, 9. https://doi.org/10.1016/j.heliyon.2023.e14559

Saaty, T.L. (1977). A Scaling Method for Priorities in Hierarchical Structures. Journal of Mathematical Psychology, 15, 234-281. https://doi.org/10.1016/0022-2496(77)90033-5

Saaty, T. L. (1980). The Analytic Hierarchy Process: Planning, Priority Setting, Resource Allocation. McGraw-Hill.

Saddam, M., Hossain, K., Mollick, P., Salauddin, M., Roy, S., Ahmad, A., Bhowmick, R., and Rony, M. (2025). Shoreline dynamics in response to sea-level changes on the eastern coast of Bangladesh. Environmental Monitoring and Assessment, 197. https://doi.org/10.1007/s10661-025-14375-x

Saleem, N., Huq, M., Twumasi, N., Javed, A., and Sajjad, A. (2019). Parameters Derived from and/or Used with Digital Elevation Models (DEMs) for Landslide Susceptibility Mapping and Landslide Risk Assessment: A Review. ISPRS Int. J. Geo Inf., 8(12), 545. https://doi.org/10.3390/ijgi8120545

Sami, M., Hoque, M., Moniruzzaman, M., and Pradhan, B. (2024). Spatial landslide risk assessment in a highly populated Rohingya refugee settlement area of Cox's Bazar, Bangladesh. Asian Geographer, 42, 79 - 100. https://doi.org/10.1080/10225706.2024.2362638

Skilodimou, H., Bathrellos, G., Koskeridou, E., Soukis, K., and Rozos, D. (2018). Physical and Anthropogenic Factors Related to Landslide Activity in the Northern Peloponnese, Greece. Land, 7(3), 85. https://doi.org/10.3390/land7030085

Suhan, M., and Adhikary, S. (2025). Exploring Climate Change Trends in Temperature and Rainfall across the Southeastern Coastal Area of Bangladesh. Journal of Engineering Science, 15(2), 51-67. https://doi.org/10.3329/jes.v15i2.82162

Sultana, N. (2020). Analysis of landslide-induced fatalities and injuries in Bangladesh: 2000-2018. Cogent Social Sciences, 6. https://doi.org/10.1080/23311886.2020.1737402

Sultana, N., Tan, S., and Hossen, M. (2024). Landslide risk assessment by integrating hazards and vulnerability indices in Southeast Bangladesh. International Journal of Disaster Risk Reduction. https://doi.org/10.1016/j.ijdrr.2024.104991

Tian, H., Gan, J., Jiang, H., Tang, C., Luo, C., Wan, C., Xu, B., Gui, F., Liu, C., and Liu, N. (2020). Failure Mechanism and Kinematics of the Deadly September 28th 2016 Sucun Landslide, Suichang, Zhejiang, China. Advances in Civil Engineering. https://doi.org/10.1155/2020/8828819

Turner, A. (2018). Social and environmental impacts of landslides. Innovative Infrastructure Solutions, 3, 1-25. https://doi.org/10.1007/s41062-018-0175-y

Varnes, D. (1978). SLOPE MOVEMENT TYPES AND PROCESSES. Transportation Research Board Special Report, 11-33.

Wang, Q., and Li, W. (2017). A GIS-based comparative evaluation of analytical hierarchy process and frequency ratio models for landslide susceptibility mapping. Physical Geography, 38, 318 - 337. https://doi.org/10.1080/02723646.2017.1294522

Wubalem, A. (2020). Landslide susceptibility mapping using statistical methods in Uatzau catchment area, northwestern Ethiopia. Geoenvironmental Disasters, 8, 1-21. https://doi.org/10.1186/s40677-020-00170-y

Wubalem, A. (2021). Landslide Inventory, Susceptibility, Hazard and Risk Mapping. Landslide. https://doi.org/10.5772/intechopen.100504

Yang, W. C., Kang, H. S., Ri, G. S., and Kim, J. S. (2022). Consistency improvement method of pairwise matrix based on consistency ratio decreasing rate and attribute weighting method considered decision makers' levels in analytic hierarchy process: application to hip joint prosthesis material selection. Mathematical Problems in Engineering, 2022(1), 1463006. https://doi.org/10.1155/2022/1463006